Synthesis and Structural Properties of Tungsten Disulfide as Transition Metal Dichalcogenides

Sundus Shawkat Abrahim[1,2] and Ziad T. Khodair[1]
[1]*Department of Physics, College of Science, University of Diyala, 32001 Baqubah, Diyala, Iraq*
[2]*Department of Information Systems and Technologies in Transport, Tashkent State Transport University, Temiryolchilar Str. 1, 100167 Tashkent, Uzbekistan*
sundusshawkat@gmail.com , ziad_tariq70@yahoo.com

Keywords: Tungsten Disulfide, Sol-Gel, X-Ray Diffraction, FESEM and FTIR.

Abstract: This study involved the synthesis of tungsten disulfide nanoparticles (WS_2) by the sol-gel process. X-ray diffraction (XRD), field emission scanning electron microscopy (FESEM), and Fourier transform infrared spectroscopy (FTIR) techniques were employed to analyze the results. XRD indicated that the nanoparticles have a hexagonal morphology, and the Scherrer equation was employed to ascertain the average crystallite size (D_{av}) of the synthesized nanoparticles, around 39 nm. FESEM images reveal that the crystalline structures exhibit heterogeneity in size and shape, with WS_2 nanosheets aggregating to create a substantial block characterized by varied interior thicknesses. The mean size distribution of WS_2 is approximately 39 nm. These findings align with the X-ray diffraction data. FTIR analysis of WS_2 nanoparticles showed that the (W-S) bond is represented by the bands at 572.71 cm^{-1} and 2924.15 $cm^{-1,}$ whereas the strong and weak absorption bands of the (S-S) bond are located at 494.4 cm^{-1} and within the range of 571.71-769.36 $cm^{-1.}$ The bands at 3740.65 cm^{-1} and 1625.21 cm^{-1} represent the (O-H) bond results.

1 INTRODUCTION

A group of thin film semiconductors known as two-dimensional transition metal dichalcogenides (TMDs) is defined by the general formula (MX_2), where M denotes transition metals (such as molybdenum, tungsten, vanadium, and zirconium) and X denotes an atom of chalcogen (such as sulfur, selenium, and tellurium). The compound consists of layers of chalcogen atoms sandwiched between the transition metal layer, as shown in Figure 1.

This family of materials has unique electronic, optical and catalytic properties, so it has a wide range of applications such as energy, environment and biomedicine [1]-[3]. Tungsten sulfide (WS_2) is a transition metal chalcogenide [4]. WS_2 occurs in the form of inorganic fullerene-like (IF-WS_2) structures and other two-dimensional structures, such as nanotubes and nanosheets [5]. These structures consist of two-dimensional molecular sheets held together by van der Waals forces. Figure 2 shows crystal structure of WS_2. Therefore, WS_2 nanoparticles have unique properties, such as lubricity, mechanical strength, and potential applications in tribology, electronics, energy storage, and other fields [6]. To prepare WS_2 nanoparticles, there are several techniques including (chemical vapor deposition, mechanical activation method, pulsed laser deposition (PLD), sol-gel method [7]-[8]. In this study, WS_2 nanoparticles were prepared by sol-reaction method, and the structural properties were studied using XRD and FESEM techniques.

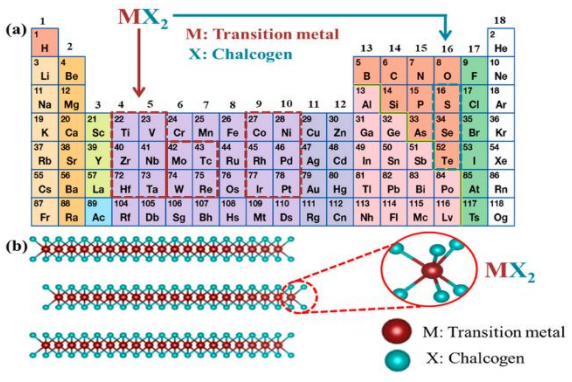

Figure 1: TMDs materials consist of 16 transition metals and three chalcogen atoms [9].

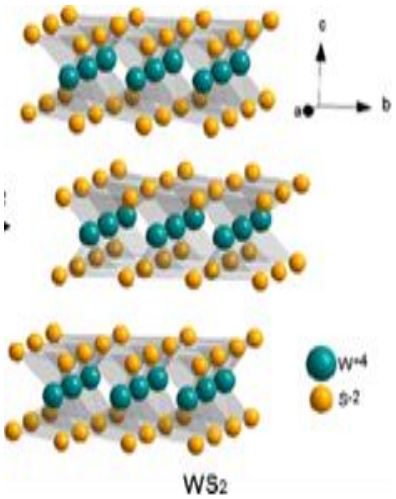

Figure 2: Crystal Structure of WS_2 [9].

2 EXPERIMENTAL DETAILS

WS_2 nanoparticles were prepared by sol-gel method by following the following steps:

1) A concentration of 0.1 M was used to dissolve sodium tungstate dehydrate, which has a molecular weight of 329.86 g/mol and a density of 2.23 g/cm^3. This substance was dissolved in deionized distilled water. There was also the utilization of thiourea (SC(NH2)2, and possessed a molecular weight of 12.76 g/mol, a purity of 99%, and a concentration of 0.1 M. There was also the addition of citric acid, which had a chemical formula of C6H8O7, a concentration of 0.5 M, and a molecular weight of 192.123 g/mol.
2) After the dissolving process was done, the acidity (pH) of the solution was found to be 1.4. It was neutralized by adding drops of ammonia solution (NH4OH) with a strength of 25%, the drops were added to the ready solution at regular times. The solution stayed on the magnetic mixer until it turned white and the pH level was equal to 7.
3) Once the solution had reached a neutral state, the temperature of the magnetic mixer was increased until the solution reached a temperature of 80 degrees Celsius. The temperature remained the same, and the solution was kept on the magnetic mixer for forty to fifty minutes. This allowed the liquid to gradually evaporate and transform into (Gel).
4) To eliminate any liquids or water molecules, the particles were annealed for two hours at 500°C in an electric furnace. Then, as illustrated in Figure 3, the particles were put into the furnace for two hours, and then for twenty-four hours until the temperature was close to room temperature, at which point (WS_2) particles were produced. Before sintering, wear (a) a solution; (b) a powder; and (c) powder nanoparticles (WS_2).

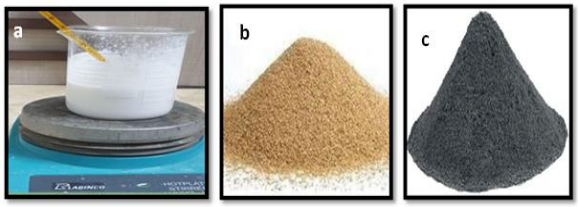

Figure 3: Steps for preparing WS_2 nanoparticles by sol-gel method wear a) show solution, b)as a powder before sintering, c) powder nano particles (WS_2) particles after sintering.

3 RESULTS AND DISCUSSIONS

3.1 Results of XRD

Figure 4 presents the XRD pattern of the synthesized WS_2 nanoparticles. The diffraction peaks 2Θ~14.33°, 28.98°, 32.52°, 33.51°, 39.56°, 44.14°, 49.82°, 58.38°, 60.40° and 76.01°, have appeared. Miller index-favored directions describe it. (002), (004), (100), (101), (103), (006), (105), (110), (112), (116), and (118), respectively. These results were found to be largely consistent with the International Data Card (ICDD card no. (00-008-0237) belonging to (WS_2) [10]. In addition, the results indicated the hexagonal structure of the nanoparticles. The large number of peaks indicates that the prepared grains are polycrystalline [11]. The distance between interplanar spacing (d_{hkl}) with the same Miller's coefficients ($_{hkl}$) was found using Brack's law and the relation (1) [8]. "d_{hkl}" was found to be close to and match the number on the WS_2 standard card (ICDD card no. 00-008-0237) [12]:

$$n\lambda = d_{hkl} \sin \Theta_B. \quad (1)$$

Where, d_{hkl} : The distance between interplanar spacing, Θ_B: Brack angle, λ: wavelength, n: order of reflection.

For the produced WS_2 nanoparticles, the crystal lattice constants (ao = bo, and co) were computed using the hexagonal structure relation (2) [13]. Table 1 displays these values.

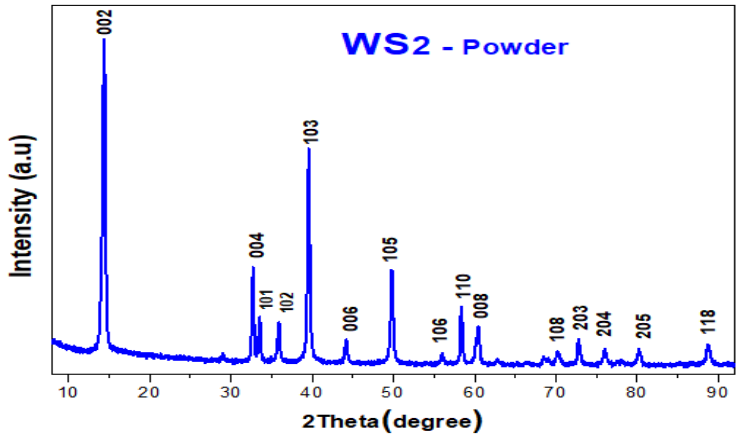

Figure 4: XRD of WS_2 nanoparticles.

$$\frac{1}{d^2{}_h} = \frac{4}{3}\left(\frac{h^2+hk+k^2}{a_o^2}\right) + \frac{l^2}{c_o^2}. \qquad (2)$$

The Miller coefficients *h*, *k*, and *l* were used to calculate the lattice constants ao and co, which were obtained from the planes (002) and (103), respectively. The lattice constant values were found to be consistent with those in the WS_2 standard card (ICDD No. 08-0237). These data are presented in Table 1. The Scherrer method was employed to determine the average crystallite size (D_{av}) of the nanoparticles that were prepared, as outlined in (3) [14]-[16].

$$D_{av} = \kappa\lambda / (\beta \cos \theta_B). \qquad (3)$$

The symbol β represents the full width at half maximum (FWHM), whereas θ_B represents the Bragg's diffraction angle. The symbol κ represents the shape factor, and λ represents the wavelength of the X-ray that is diffractioning the sample. As can be seen in Table 1, the crystallite size of the nanoparticles that were formed was determined to be about 22 nanometers. The dislocation density (δ) is a measurement that is used to determine the amount of defects present in the crystal. The lowest dislocation density value that was discovered in this work provided evidence that the sol-gel method was successful in producing WS_2 nanoparticles that had demonstrated good crystallization. Formula 4 was utilized in order to calculate the dislocation density [17], which may be found in Table 1.

$$\delta = 1 / D^2_{av} \qquad (4)$$

A definition of specific surface area (SSA) is the area represented in mass units (m^2/g). It ascertains material quality and constitutes a significant attribute of nanoparticles. It also provides information about superficial encounters [17]. Table 1 presents the SSA values obtained by 5 [17]:

$$SSA = S_V / \rho . \qquad (5)$$

To find the surface density (SV), we need to take the number of K_{SV} (which is 6 for a sphere) and D_{av}. The material density for WS_2 nanoparticles is ρ, which is 7.5 g/cm^3, i.e., SV = . Rearranging (5) yields the following (6):

$$SSA = 6 \times 10^3 / (D_{av}\, \rho) \qquad (6)$$

3.2 Analysis of FESEM

The WS_2 nanoparticles synthesized with sol-gel were analyzed using FESEM. The crystals in Figure 5a and 5b are of different sizes and shapes, and the WS_2 nano sheets can be stacked to make a big block with different thicknesses inside. The findings here are in agreement with those of studies [18]-[20]. The size range of WS_2 is shown in Figure 5b. It is about 42 nm on average.

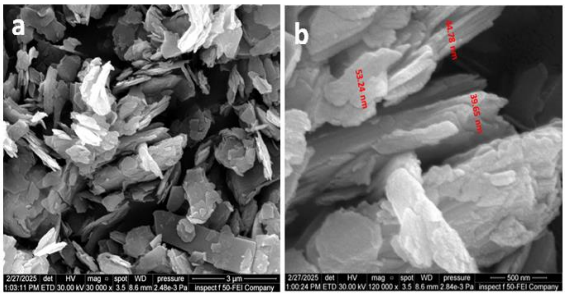

Figure 5: FESEM image of WS_2 nanoparticles: a and b.

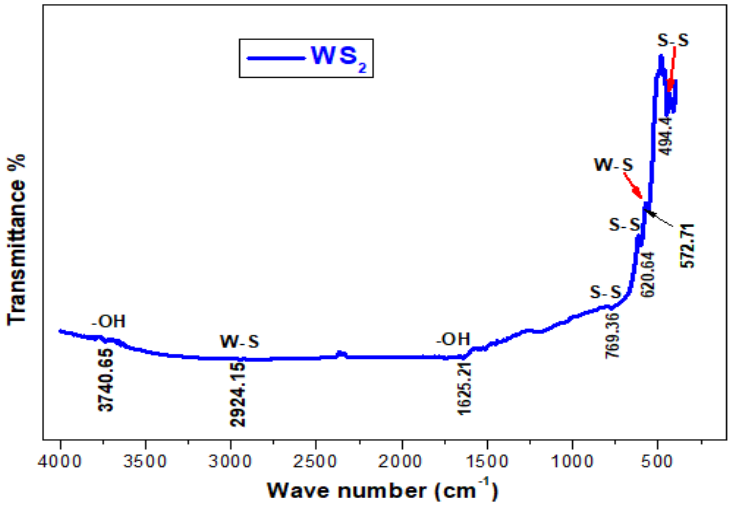

Figure 6: FTIR measurements for WS2 nanoparticles.

Table 1: Hexagonal structure relation.

θ°	d-spacing (Å)	FWHM (rad)	average crystallite size (D_{av}) (nm)	Micro Strain $*10^{-3}$	Dislocation density (δ) nm^{-2}	SSA ($m^2.g^{-1}$)
14.33	6.1666	0.3464	23	0.45775	0.00189	35
28.98	3.0808	0.5196	16	0.37711	0.00390	50
32.52	3.0792	0.3464	24	0.41297	0.00174	33
33.51	2.6735	0.3464	24	0.41297	0.00174	33
39.56	2.2779	0.5196	16	0.28549	0.00390	50
44.17	2.0504	0.3464	25	0.40511	0.00160	32
49.82	1.8303	0.3464	25	0.33445	0.00160	32
58.38	1.5806	0.5196	18	0.181	0.003086	45
60.40	1.5324	0.5196	18	0.44459	0.003086	15
76.01	1.2519	0.3464	29	0.23658	0.001189	28

3.3 FTIR Measurements

Fourier transform infrared (FTIR) measurements were performed for WS_2 nanoparticles prepared by the sol-gel method in the range of 400-4000 cm^{-1}. The transmittance spectrum was measured as a function of wavenumber. The transmittance spectrum was also measured as a function of wavenumber. Figure 6 shows relatively strong absorption bands at wavelengths of 494.4, 572.71, 620.64, 769.36, 1625.21, 2925.15, and 3740.65 cm^{-1}. These results are consistent with studies [21]-[25] which showed that the strong and weak absorption bands of the (S-S) bond are located at 494.4 cm^{-1} as well as between 571.71-769.36 cm^{-1}, While the bands located at 572.71 and 2924.15 cm^{-1} are due to the (W-S) bond. While the bands located at 1625.21 and 3740.65 cm^{-1} are due to the (O-H) bond.

4 CONCLUSIONS

The sol-gel method was used to make transition metal dichalcogenides (WS2) nanoparticles by mixing sodium tungstate dehydrate [Na2WO4.2H2O] with thiourea (SC(NH2)2). The XRD study gave us nanoparticles with an average particle size of (39 nm). These results were the same as the particle size we got from the FESEM images, which was about (42 nm).

These findings align with the X-ray diffraction data. FTIR analysis of WS2 nanoparticles showed that the (W-S) bond is represented by the bands at 572.71 cm^{-1} and 2924.15 cm-1, whereas the strong and weak absorption bands of the (S-S) bond are located at 494.4 cm-1 and within the range of 571.71-769.36 cm^{-1}. The bands at 3740.65 cm^{-1} and 1625.21 cm^{-1} represent the (O-H) bond results.

REFERENCES

[1] S. Gupta, J.J. Zhang, J. Lei, H. Yu, M. Liu, X. Zo, and B.I. Yakobson, "Two-Dimensional Transition Metal Dichalcogenides: A Theory, and Simulation Perspective," Chemical Reviews, 2025.

[2] K.B. Ibrahim, T.A. Shifa, S. Zorzi, M.G. Sendeku, E. Moretti, and A. Vomiero, "Emerging 2D materials beyond mxenes and TMDs: Transition metal carbo-chalcogenides," Progress in Materials Science, p.101287, 2024.

[3] R. Sharma, R. Laishram, B.K. Gupta, R. Srivastva, and O.P. Sinha, "A review on MX2 (M= Mo, W and X= S, Se) layered material for opto-electronic devices," Advances in Natural Sciences: Nanoscience and Nanotechnology, vol. 13, no. 2, p.023001, 2022.

[4] S. Niknam, S.A. Dehdast, O. Pourdakan, M. Shabani, and M.K. Koohi, "Tungsten disulfide nanomaterials (WS2 NM) application in biosensors and nanomedicine: a review," Nanomedicine Research Journal, vol. 7, no. 3, pp.214-226, 2022.

[5] L. Yue, D. Xu, Z. Wei, T. Zhao, T. Lin, R. Tenne, A. Zak, Q. Li, and B. Liu, "Size and shape's effects on the high-pressure behavior of WS2 nanomaterials," Materials, vol. 15, no. 8, p.2838, 2022.

[6] T. Ouyang, W. Tang, W. Lei, and L. Cheng, "Tribological and friction-induced vibration behaviors of inorganic fullerene-like tungsten disulfide and three-dimensional graphene as lubricant additives," Journal of Tribology, vol. 145, no. 3, p.031701, 2023.

[7] S.J. Hazarika and D. Mohanta, "Revealing mechanical, tribological, and surface-wettability features of nanoscale inorganic fullerene-type tungsten disulfide dispersed in a polymer," Journal of Materials Research, vol. 34, no. 21, pp.3666-3677, 2019.

[8] X. Lin, Y. Liu, K. Wang, C. Wei, W. Zhang, Y. Yan, Y.J. Li, J. Yao, and Y.S. Zhao, "Two-dimensional pyramid-like WS2 layered structures for highly efficient edge second-harmonic generation," ACS Nano, vol. 12, no. 1, pp.689-696, 2018.

[9] Z. Li and S.L. Wong, "Functionalization of 2D transition metal dichalcogenides for biomedical applications," Materials Science and Engineering: C, vol. 70, pp.1095-1106, 2017.

[10] S. Bobba, F.A. Deorsola, G.A. Blengini, and D. Fino, "LCA of tungsten disulphide (WS2) nano-particles synthesis: state of art and from-cradle-to-gate LCA," Journal of Cleaner Production, vol. 139, pp.1478-1484, 2016.

[11] I. Hotovy, L. Spiess, M. Mikolasek, I. Kostic, M. Sojkova, H. Romanus, M. Hulman, D. Buc, and V. Rehacek, "Layered WS2 thin films prepared by sulfurization of sputtered W films," Applied Surface Science, vol. 544, p.148719, 2021.

[12] S.M. Jassim, A.A. Mohammed, M.M. Kareem, and Z.T. Khodair, "Synthesis and characterization of Cr-doped cadmium oxide thin films for NH3 gas-sensing applications," Bulletin of Materials Science, vol. 47, no. 2, p.104, 2024.

[13] A.M. Mohammad, H.S. Ahmed Al-Jaf, H.Sh. Ahmed, M.M. Mohammed, and Z.T. Khodair, "Structural and morphological studies of ZnO nanostructures," Journal of Ovonic Research, vol. 18, no. 3, pp.443-452, 2022.

[14] A.A. Mohammed, M.A. Ahmed, and S.M. Jassim, "Preparation and investigation of the structural and optical characteristics of manganese-doped cadmium oxide films," Digest Journal of Nanomaterials & Biostructures (DJNB), vol. 18, no. 2, pp.613-625, 2023.

[15] S.A. Hameed, M.M. Kareem, Z.T. Khodair, and I.M.M. Saeed, "The influence of deposition temperatures on the structural and optical properties for NiO nanostructured thin films prepared via spray pyrolysis technique," Chemical Data Collections, vol. 33, p.100677, 2021.

[16] K. Hameed, "A state space approach via Discrete Hartley transform of type and For the solution of the State model of Linear time-invariant systems (L.T.I.S's.)," IJApSc, vol. 2, no. 1, pp.53-60, Mar. 2025, [Online]. Available: https://doi.org/10.69923/k1qp1d65.

[17] Mahmood, "Evaluating Radioactivity Levels and Determining Risk Indicators in Plant Samples in Kirkuk-Iraq," IJApSc, vol. 1, no. 3, pp.25-34, Dec. 2024, [Online]. Available: https://doi.org/10.69923/m7spn227.

[18] R. Leelavathi, K. Vivekanandan, V. Hariharan, and R. Abirami, "Identifying the Suitability of MoS2 Nanoparticles by Two Different Methods for Photo Catalytic Applications," International Journal of Nanoscience, vol. 22, no. 2, p.2350006, 2023.

[19] S.N.A. Shah, S. Shahabuddin, M.F.M. Sabri, M.F.M. Salleh, S.M. Said, and K.M. Khedher, "Thermal conductivity, rheology and stability analysis of 2D tungsten disulphide-doped polyaniline-based nanofluids: An experimental investigation," International Journal of Energy Research, vol. 45, no. 2, pp.1550-1575, 2021.

[20] S. Singh, S. Sharma, B.S. Bajwa, and I. Kaur, "Tungsten disulfide (WS2) nanosheets: synthesis, characterization, adsorption studies and application for remediation of groundwater samples with high prevalence of uranium from Faridkot district of SW-Punjab," Journal of Radioanalytical and Nuclear Chemistry, vol. 330, no. 3, pp.1425-1436, 2021.

[21] M. Latha and J.V. Rani, "WS2/graphene composite as cathode for rechargeable aluminum-dual ion battery," Journal of The Electrochemical Society, vol. 167, no. 7, p.070501, 2019.

[22] S. Majumder, M. Shao, Y. Deng, and G. Chen, "Two dimensional WS2/C nanosheets as a polysulfides immobilizer for high performance lithium-sulfur batteries," Journal of The Electrochemical Society, vol. 166, no. 3, pp.A5386-A5395, 2019.

[23] G.I. Dovbeshko, U.K. Afonina, M.V. Olenchuk, I.M. Kupchak, O.P. Gnatyuk, G.P. Monastyrskyi, A.S. Nikolenko, H.V. Shevliakova and A.N. Morozovska, "Effect of 2D-WS2 Nanoparticles on a Local Electrical Field at a Membrane Vicinity: Vibrational Spectroscopy Data," The Journal of Physical Chemistry C, vol. 128, no. 3, pp.1131-1138, 2023.